JID Open

Proteome Profiling of Human Cutaneous Leishmaniasis Lesion

Claire da Silva Santos[1], Sanaz Attarha[2], Ravi Kanth Saini[2], Viviane Boaventura[3], Jackson Costa[1], Ricardo Khouri[1], Manoel Barral-Netto[1,3,4], Cláudia Ida Brodskyn[1,4,5] and Serhiy Souchelnytskyi[2]

In this study, we used proteomics and biological network analysis to evaluate the potential biological processes and components present in the identified proteins of biopsies from cutaneous leishmaniasis (CL) patients infected by *Leishmania braziliensis* in comparison with normal skin. We identified 59 proteins differently expressed in samples from infected and normal skin. Biological network analysis employing identified proteins showed the presence of networks that may be involved in the cell death mediated by cytotoxic T lymphocytes. After immunohistochemical analyses, the expression of caspase-9, caspase-3, and granzyme B was validated in the tissue and positively correlated with the lesion size in CL patients. In conclusion, this work identified differentially expressed proteins in the inflammatory site of CL, revealed enhanced expression of caspase-9, and highlighted mechanisms associated with the progression of tissue damage observed in lesions.

Journal of Investigative Dermatology advance online publication, 16 October 2014; doi:10.1038/jid.2014.396

INTRODUCTION

Leishmaniasis affects millions of individuals worldwide, causing serious morbidity and mortality (Kedzierski, 2010). Human cutaneous leishmaniasis (CL) caused by *Leishmania braziliensis* is characterized by the development of a single lesion at the site of the sand fly bite, strong cellular responses, and scarce numbers of parasites in the lesions (Carvalho *et al.*, 2012). The presence of activating cytokines, such as IFN-γ and tumor necrosis factor-α, is decisive for the control of parasite dissemination, but an exaggerated T helper type 1 cell response and the presence of cytotoxic CD8 T cells have been associated with severe inflammation and tissue destruction in CL lesions (Faria *et al.*, 2009, Novais *et al.*, 2013; Santos, Cda *et al.*, 2013).

Proteomics can provide a global and comprehensive approach to the identification and description of biochemical processes, pathways, and networks at the protein level. Several proteomic studies focusing on *Leishmania* infection have explored aspects related to parasite biology and *Leishmania*–host cell interactions (Forgber *et al.*, 2006; Rukmangadachar *et al.*, 2011; Matrangolo *et al.*, 2013; Menezes *et al.*, 2013). This study attempts to employ large-scale proteomic analysis to identify differences in protein expressions in the lesions of patients. We identify 59 differentially expressed proteins between lesion from CL patients and normal skin using two-dimensional gel electrophoresis (2DE) coupled with mass spectrometry (MS). Computational approaches of the biological network formed by identified proteins highlighted pathways that may be involved in the apoptosis, cell proliferation, and cell-cycle mechanisms. Immunohistochemical analyses validated the presence and involvement of caspase-9, caspase-3, and granzyme B in the tissue injury in CL patients.

RESULTS

Proteome profiling of lesions from CL patients

Proteomic analysis was performed to investigate differentially expressed proteins between lesions from CL patients and normal skin. Histological analysis of CL samples showed that the inflammatory infiltrate did not vary in composition among the biopsies with the presence of lymphocytes, macrophages, and plasma cells. The presence of focal necrosis in the biopsies was also noticed (data not shown). Total protein extracts obtained from each sample were separated by 2DE and visualized by silver nitrate staining. Protein profiles from the two groups of samples (CL lesions and normal skin) were compared using the Image Master 2D platinum software. Images of representative 2D gels are shown in Figure 1. In each CL sample, spot detection revealed a mean of 489 protein spots (489 ± 135 per gel), and in normal skin samples a mean of 481 protein spots (481 ± 96 per gel) was observed.

Three replicates of 2DE gels were performed for each sample with reproducible results, indicating that technical variability was low. The biological variation between samples

[1]*Centro de Pesquisas Gonçalo Moniz, Fundação Oswaldo Cruz (FIOCRUZ), Salvador, Brazil;* [2]*Department of Oncology-Pathology, Karolinska Institutet, Stockholm, Sweden;* [3]*Faculdade de Medicina da Bahia, Universidade Federal da Bahia, Salvador, Brazil;* [4]*Instituto de Investigação em Imunologia, São Paulo, Brazil and* [5]*Instituto de Ciências da Saúde, Universidade Federal da Bahia, Salvador, Brazil*

Correspondence: Claire da Silva Santos or Cláudia Ida Brodskyn, Laboratório Integrado de Microbiologia e Imunorregulação, Centro de Pesquisas Gonçalo Moniz, Rua Waldemar Falcão, 121, Candeal, Salvador, Bahia 40295-001, Brazil. E-mail: cler_ss@hotmail.com or brodskyn@bahia.fiocruz.br

Abbreviations: CL, cutaneous leishmaniasis; 2DE, two-dimensional gel electrophoresis; MS, mass spectrometry

Received 14 May 2014; revised 29 July 2014; accepted 7 August 2014; accepted article preview online 10 September 2014

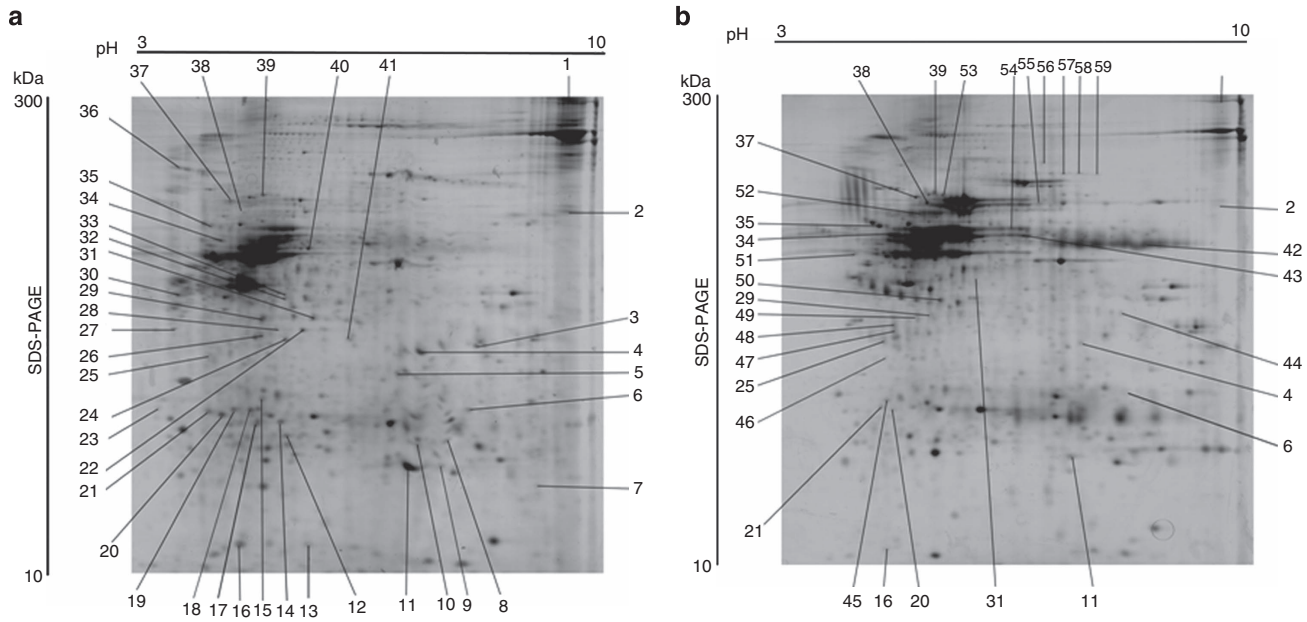

Figure 1. Images of representative 2D gels. The images are representative of six samples showing separation of proteins extracted from lesions of (**a**) cutaneous leishmaniasis (CL) patients and (**b**) normal skin. Directions of isoelectric focusing and SDS-PAGE are indicated on the top and on the side of the left gel image. Spots marked only in gel (**a**) indicate protein spots unique in the CL samples. Spots marked only in gel (**b**) show the protein spots unique in normal skin. Spots marked in gels (**a**, **b**) indicate protein spots differently regulated between the samples. The protein spots were identified by matrix-assisted laser desorption/ionization time of flight (MALDI-TOF) mass spectrometry. List of identified proteins is given in Table 1.

in each group was <40%, meaning >60% of coincident matched spots in each group. Silver-stained protein spots were distributed in all areas of the pH gradient (pH 3–10), and an approximately even distribution was found for proteins in the range of molecular masses from 25 to 100 kDa. The overall distribution of proteins in 2DE gels was similar to proteome patterns observed for other reported studies of the skin (Haudek *et al.*, 2009; Ong *et al.*, 2010; Javad and Day, 2012). For identification of differentially expressed proteins, protein spots that showed >2-fold difference in expression between the group of CL and normal skin samples were selected for further analysis. A total of 150 differentially expressed spots were excised from 2DE gels from CL or normal skin samples. Identification was performed by matrix-assisted laser desorption/ionization time-of-flight MS. In all, 59 proteins were identified unambiguously, whereas MS of proteins from other spots did not provide secured identification. Among the 59 identified proteins, 29 spots were unique in CL patients (marked spots just in the Figure 1a), 17 were unique in normal skin (marked spots just in Figure 1b), and 9 were upregulated and 4 were downregulated spots of CL biopsies related to normal skin (marked spots in both Figure 1a and b). The protein spots were labeled numerically and corresponded to the protein identifications listed in Table 1. There are relatively high proportions of unique proteins for CL or normal skin as compared with up- or downregulated proteins. This level of expression of proteins might indicate that CL may lead to rather significant changes in regulatory mechanisms at the sites of infection.

Biological network analysis of identified proteins

To explore biological processes and functions that could be mediated by the 59 identified proteins, we performed a computational study using GoMiner, Cytoscape, and IPA-Ingenuity Systems analysis. The GoMiner tool clustered identified proteins into hierarchical categories based on biological process and molecular function. Analysis of intracellular mechanisms showed that the identified proteins were involved in regulation of cell death (SKIL, KPNA1, CDK11A, and CASP-9), cell adhesion (BCAM, SPECC1, and DCHS2), cell cycle (CDK11A, NEK11, HAUS5, ANKLE2, and CENP-E), immune response (TRB, KIR2DL4, IL12RB1, and GNL1), and homeostasis (SLC8A1 and ATP1A2). A Venn diagram was constructed to identify common and exclusively regulated biological processes (Kestler *et al.*, 2005). We found a number of proteins that are expressed by the two samples, suggesting common mechanisms between CL lesions and normal skin (Figure 2c). Some of the common biological functions observed were apoptosis (CASP-9), immune response (TRB), and biosynthetic process (BRF1) that were upregulated in CL biopsies. In fact, there is a recruitment of T cells to the infection site that could be reflected by an increase in the expression of TRB (Clarêncio *et al.*, 2006; Keesen *et al.*, 2011). The inflammatory response observed in the lesions led to an increase in apoptotic process, represented by an increase in CASP-9. In addition, some proteins were exclusively expressed in CL biopsies (Figure 2a) or normal skin samples (Figure 2b).

To explore the mechanisms represented by the identified proteins, we generated networks of interactions between the

Table 1. Proteins differently expressed between lesions from CL patients and normal skin

Spot no.	Gene Ontology	Protein name	NCBI accession no.	Theoretical value MW (kDa)	Theoretical value pI	Experimental value[1] MW(kDa)	Experimental value[1] pI	Probability	Z-value	Matched peptide	Coverage (%)	Expression change
1	TTC37	Tetratricopeptide repeat domain 37	7662078	177.5	7.7	210	9.5	1.0e+000	2.24	14	13	Upregulated
2	FBF1	Fas (TNFRSF6) binding factor 1	23270771	90.58	6.7	100	9.5	9.0e-001	1.05	8	11	Upregulated
3	CDK11A	Cyclin-dependent kinase 11A	66267414	53.91	4.8	51	8.2	1.0e+000	2.24	4	13	Unique CL
4	AIDA	Chromosome 1 open reading frame 80	119626771	35.08	6.2	55	7.3	1.0e+000	2.43	6	18	Upregulated
5	FAM13C	FAM13C	119574574	55.44	6.5	50	6.8	1.0e+000	2.43	11	16	Unique CL
6	CASP9	Caspase-9	158257592	47.09	5.7	40	8.3	1.0e+000	2.43	4	11	Upregulated
7	RABL2A	RAB, member of RAS oncogene family-like 2A	220675523	18.52	4.4	25	9.2	1.0e+000	2.34	4	27	Unique CL
8	TMEM40	Transmembrane protein 40	31542667	25.59	5.3	37	8.2	1.0e+000	2.43	4	23	Unique CL
9	GAPVD1	GAPVD1	21739944	38.70	6.3	30	7.8	9.0e-001	1.57	6	15	Unique CL
10	IGBP1	Immunoglobulin (CD79A) binding protein 1	193786113	39.28	5.2	36	7.3	1.0e+000	2.43	7	22	Unique CL
11	MIF4GD	MIF4G domain-containing protein isoform 1	335334986	30.70	5.2	30	7.2	1.0e+000	2.42	5	21	Upregulated
12	BBOX1	Gamma-Butyrobetain, 2-Oxoglutarate Dioxygenase 1	295982624	45.30	6.3	35	5.5	1.0e+000	2.43	6	19	Unique CL
13	AKIR1N1	AKIR1N1	119627688	18.01	7.2	15	5.8	1.0e+000	2.25	4	35	Unique CL
14	CHKA	Choline kinase-α	118137437	45.59	6.5	41	5.4	1.0e+000	2.41	7	19	Unique CL
15	METTL10	METTL10	57997124	32.13	5.8	5.0	4.3	1.0e+000	2.05	7	14	Unique CL
16	TRB	TCR-β	54292535	5.58	6.8	17	4.5	1.0e+000	2.43	4	46	Upregulated
17	HAGH	HAGH	158261333	29.19	6.5	33	4.7	1.0e+000	2.43	5	27	Unique CL
18	IL12RB1	Interleukin-12 receptor subunit beta-1	24497440	43.38	6.8	40	4.5	1.0e+000	2.43	9	28	Unique CL
19	SNRNP48	SNRNP48	11957561	41.82	6.0	33	4.0	1.0e+000	1.30	6	11	Unique CL
20	BRF1	Transcription factor IIIB 90 kDa	338753412	48.36	4.8	36	3.9	1.0e+000	2.43	7	17	Upregulated
21	HAUS5	HAUS augmin-like complex subunit 5	39963101	32.91	7.2	38	3.7	1.0e+000	1.70	6	25	Unique CL
22	KIR2DL4	Killer cell receptor	39963101	36.05	6.2	55	5.5	1.0e+000	2.17	3	15	Unique CL
23	FKBP4	FKBP4	4503729	52.07	5.3	40	3.5	1.0e+000	2.43	8	16	Unique CL
24	ATL1	Atlastin GTPase 1	4406632	54.50	5.8	50	5.5	1.0e+000	2.43	4	13	Unique CL
25	BCAM	Basal cell adhesion molecule	342196430	68.17	5.5	55	3.8	1.0e+000	2.43	7	13	Downregulated
26	UBR1	Ubiquitin protein ligase E3 component n-recognin 1	14042752	95.40	5.8	55	5.0	1.0e+000	0.89	11	15	Unique CL
27	KPNA1	Karyopherin-α 1	222144293	60.95	4.9	53	3.6	1.0e+000	2.43	6	13	Unique CL
28	DARS	Aspartyl-tRNA synthetase	45439306	57.52	6.1	52	5.5	1.0e+000	2.43	8	17	Unique CL
29	cTAGE4	cTAGE family, member 4	193290160	88.31	5.2	66	5.6	1.0e+000	0.87	13	19	Upregulated
30	TBC1D9B	TBC1D9B	193786679	64.56	4.7	70	3.5	1.0e+000	1.16	7	15	Unique CL
31	ATP1A2	Na(+)/K(+)-ATPase	193785194	73.51	5.6	65	5.8	1.0e+000	2.43	7	16	Upregulated
32	RHPN2	Hypothetical protein Rhophilin-2	21732479	74.40	6.5	72	5.6	1.0e+000	2.43	5	9	Unique CL

Table 1. (Continued)

Spot no.	Gene Ontology	Protein name	NCBI accession no.	Theoretical value MW (kDa)	Theoretical value pI	Experimental value[1] MW(kDa)	Experimental value[1] pI	Probability	*Z*-value	Matched peptide	Coverage (%)	Expression change
33	SKIL	SKI-like isoform 3	223029422	76.02	6.6	75	5.6	1.0e+000	2.04	7	7	Unique CL
34	RNF40	Ring finger protein 40	7662230	114.4	6.0	90	4.2	1.0e+000	2.43	10	10	Unique CL
35	ANKLE2	Ankyrin repeat and LEM domain-containing protein 2	148664230	104.95	6.7	95	3.8	1.0e+000	1.53	7	13	Downregulated
36	MYPBC1	Hypothetical protein MYBPC1	30722349	88.87	5.9	150	3.5	1.0e+000	0.91	9	12	Unique CL
37	PDE4DIP	Phosphodiesterase 4D	30268245	114.62	5.0	90	4.5	1.0e+000	1.27	7	8	Downregulated
38	SLC8A1	SLC8A1	163914373	105.58	4.9	95	4.7	1.0e+000	1.88	5	5	Downregulated
39	SART1	Squamous cell carcinoma antigen recognized by T cells	62897593	90.42	6.0	96	5.0	1.0e+000	2.43	11	15	Unique CL
40	PTPN5	PTPN5	221039972	59.64	5.0	75	5.5	1.0e+000	2.43	7	8	Unique CL
41	NEK11	Serine/threonine-protein kinase Nek11	41281753	54.56	5.7	51	6.3	1.0e+000	2.43	6	16	Unique CL
42	ZBTB10	ZBTB10	119607481	74.92	4.8	69	8.0	1.0e+000	20.7	5	8	Unique CL
43	SNX25	SNX25	193787897	83.27	5.9	70	6.8	1.0e+000	2.43	8	14	Unique N. skin
44	SPECC1	SPECC1	21706968	55.18	5.1	64	8.2	1.0e+000	2.43	12	18	Unique N. Skin
45	CENPE	Centromere-associated protein E	67464447	39.55	7.0	40	4.5	1.0e+000	1.21	8	29	Unique N. Skin
46	UBOX5	RING finger protein 37 isoform B	40806196	54.40	6.8	45	4.0	1.0e+000	2.27	5	11	Unique N. Skin
47	GNL1	Guanine nucleotide binding protein-like 1	39645120	54.32	5.0	55	4.5	1.0e+000	2.43	6	10	Unique N. Skin
48	VPS51	VPS51	38014611	79.57	6.6	58	4.5	1.0e+000	2.43	10	10	Unique N. Skin
49	ALDH2	Mitochondrial aldehyde dehydrogenase 2	48256839	56.85	6.4	63	5.3	1.0e+000	2.43	6	15	Unique N. Skin
50	SYNE1	Nesprin-1	73909082	59.51	6.5	70	5.4	1.0e+000	2.43	8	15	Unique N. Skin
51	DCHS2	Protocadherin protein	45439306	57.52	6.1	60	3.8	1.0e+000	2.43	8	13	Unique N. Skin
52	PALD1	PALADIN	20521820	98.25	6.1	98	5.5	1.0e+000	2.43	9	17	Unique N. Skin
53	HNRNPUL2	Heterogeneous nuclear ribonucleoprotein U-like 2	118601081	85.66	4.9	90	5.3	1.0e+000	1.85	7	18	Unique N. Skin
54	ARHGEF7	Rho guanine nucleotide exchange factor (GEF) 7	55957399	71.12	6.6	72	6.3	1.0e+000	2.43	6	7	Unique N. Skin
55	CCDC114	Hypothetical protein FLJ32926	119572712	80.73	5.9	85	6.8	1.0e+000	1.53	9	17	Unique N. Skin
56	IPO7	Importin-7	5453998	120.81	4.7	130	7.0	1.0e+000	1.13	10	18	Unique N. Skin
57	STK31	Serine/threonine kinase 31	51095006a	114.25	5.0	120	7.2	1.0e+000	2.43	9	13	Unique N. Skin
58	TNS3	Tensin 3 variant	62087570	137.54	6.4	121	7.4	1.0e+000	0.92	7	10	Unique N. Skin
59	ATP2B2	ATPase, Ca^{2+} transporting, plasma membrane 3, isoform CRA_b	119593265	128.19	5.7	119	7.6	1.0e+000	2.31	9	9	Unique N. skin

Abbreviations: CL, cutaneous leishmaniasis; pI, isoelectric point, MW, molecular weight; N., normal; NCBI, National Center for Biotechnology Information.
Gene Ontology, protein name, NCBI accession number, theoretical value, probability, *Z*-value, matched peptide, and sequence coverage were obtained by search with Profound.
[1]Experimental values were calculated from migration in 2D gels. The differences observed between the experimental and theoretical MW values (4, 15, 16, 26, and 36) were possibly due to the presence of isoforms or posttranslational modification of proteins.

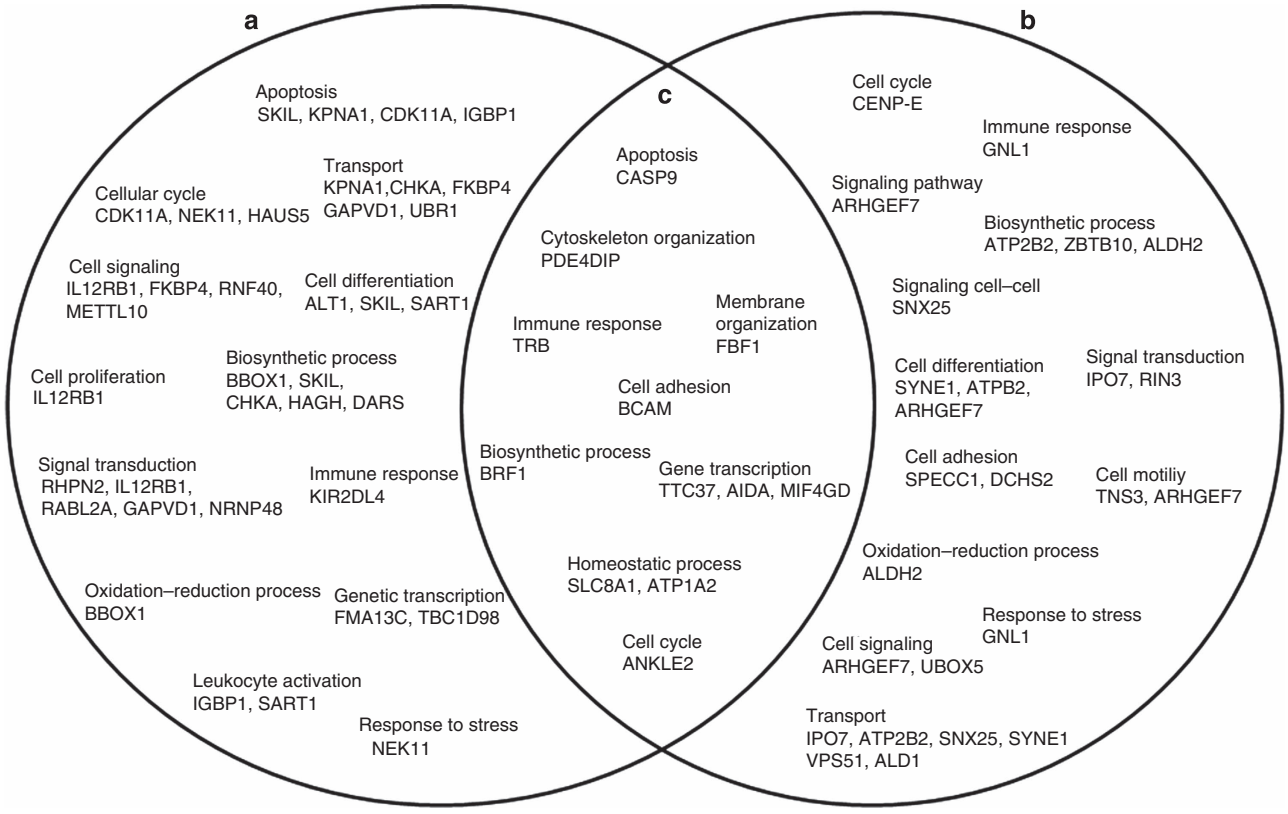

Figure 2. Schematic Venn diagram of the protein spots identified. The Venn diagram shows proteins unique to (**a**) cutaneous leishmaniasis (CL) patients, (**b**) normal skin, and (**c**) overlaps between biologic processes defined by the identified proteins between the samples. The diagram was built upon analysis of the identified proteins using a GoMiner tool. ''Biologic Process'' category was selected for the analysis of affected functions.

59 identified proteins and proteins and genes that may be affected by them. The generated network showed 505 nodes (proteins), including the 59 proteins identified by us (green diamond symbol in Supplementary Figure S1 online) and 457 proteins identified by the MiMiplugin embedded in Cytoscape software that interact with these ones (red ellipse symbol in Supplementary Figure S1 online). A number of proteins have been observed, such as IL-23, TGFBR1, TNFRI, CASP-3, CASP-8, and GZMB.

Subnetworks represent nodes with higher connectivity between them, as compared with other nodes. In order to better visualize the interactions among the proteins, 13 subnetwork modules were extracted from the whole network using a MCODE tool embedded in Cytoscape (Figure 3a and Supplementary Figure S2a–m online). The highly ranked modules represented protein associated with apoptosis (Figure 3a), cellular signaling, transcription, cell cycle, and cell proliferation (Supplementary Figure S2a–m online). Besides that, to better elucidate the interactions among the 59 proteins identified, IPA-Ingenuity Systems was employed to build a model of potential canonical networks and connections. The main canonical pathway identified involved cytotoxic T lymphocyte–mediated apoptosis of target cells (Figure 3b). This network comprised 34 proteins. Of these, 18 proteins were differentially expressed between the samples, 9 were unique to CL biopsies (SKIL, KPNA, CHKA, RNF40, ZBTB10, IL12RB1, KIR2DL4, PTPN-5, and IGBP, shown in red), 5 were upregulated (BRF1, CASP9, AIDA1, TRB, ATP1A2, shown in red), and 4 were downregulated (ALDH2, SLC8A1, TNS3, and PALD, shown in green) proteins in CL biopsies related to normal skin.

The biological network analysis performed in this study complemented the limitation of identifying only a part of the differentially expressed proteins, introducing into the analysis proteins and genes that have not been characterized or detected in 2D gels.

Validation of caspase-9, caspase-3, and granzyme B protein expression

The mechanism of tissue damage and ulceration observed in CL patients is not fully understood. The participation of molecules Fas/FasL and TRAIL (tumor necrosis factor–related apoptosis-inducing ligand) that activate the apoptosis pathway has been implicated in the development of tissue injury (Rethi and Eidsmo, 2012). It was demonstrated that the recruitment of CD8 T cells expressing granzymes to the site of infection contributes to the tissue destruction (Faria *et al.*, 2009; Santos, Cda *et al.*, 2013). Granzyme B can act at multiple points to initiate cell death. Targets of granzyme B include activation of caspase-3 directly or through the mitochondrial pathway by inducing activation of caspase-9 that in turn activates caspase-3, amplifying the caspase cascade (Lord *et al.*, 2003).

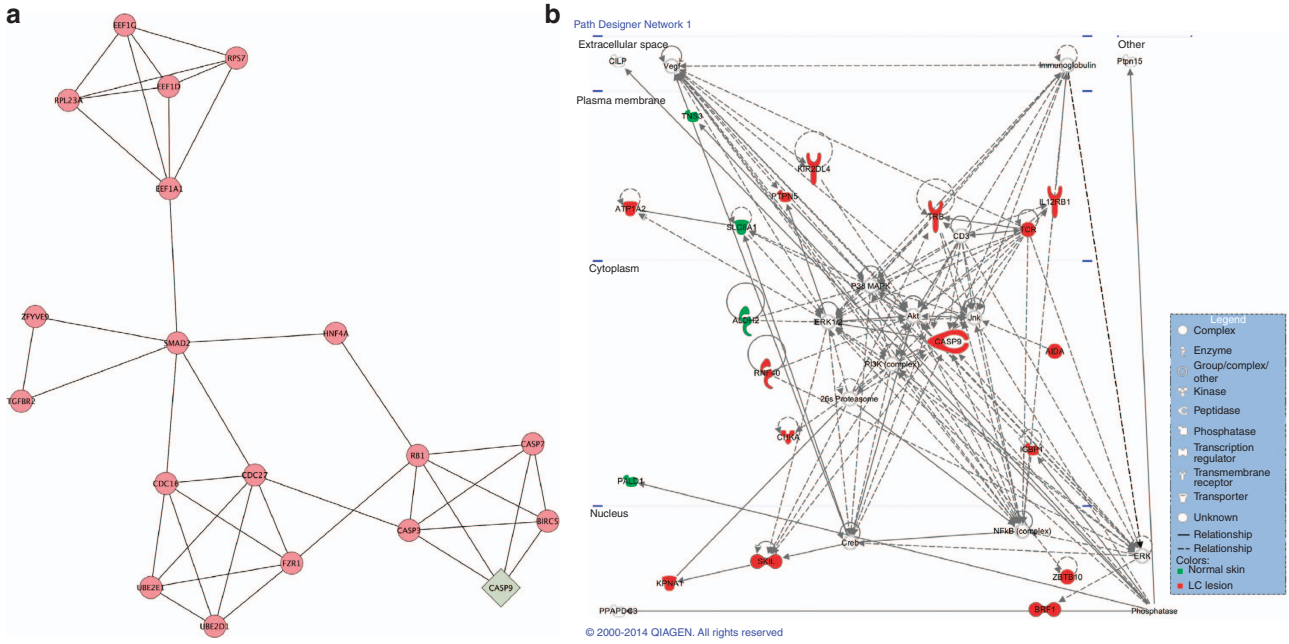

Figure 3. Network and canonical pathway built with 59 differentially expressed proteins. (**a**) Subnetwork modules associated with apoptosis extracted from the whole network using an MCODE tool. (**b**) Cytotoxic T lymphocyte–mediated apoptosis of target cell network ($P<0.003$) performed by Ingenuity Pathway analysis. The red color is an indication of the upregulated/unique proteins expressed in cutaneous leishmaniasis (CL) lesions, and green color indicates downregulated/unique proteins expressed in normal skin. Full and dashed lines represent direct and indirect interactions, respectively, between the proteins. Network shapes are represented in the legend.

Proteomic and network analysis performed in this study showed that the main canonical pathways found were associated with apoptosis.

In order to validate this analysis, pointing out apoptosis as a main canonical pathway, we explored CASP-9, CASP-3, and GZMB (granzyme B) expression, the three proteins associated with cell death pathway. CASP-9 was selected because of its upregulation in the lesions from CL patients and mainly owing to central positioning in the network obtained by IPA Ingenuity System analysis (Figure 3b). Although CASP-3 and granzyme B have not been identified in Table 1, they were observed in the whole network (Supplementary Figure S1 online). The validation was performed by immunohistochemical evaluations in biopsies from CL patients and normal skin. The expression of capase-9 (Figure 4a), caspase-3 (Figure 4c), and granzyme B (Figure 4e) was consistently higher in CL lesions than in normal skin samples, as shown in Figure 4b, d, and f. The expression of these proteins was detected mainly in mononuclear cells presented in the inflammatory infiltrate. No reactivity was detected using an isotype control antibody (Figure 4g). To further investigate the relation between the proteins identified in the proteomic analysis, correlation studies were performed. In Figure 5, we observed a positive correlation between expressions of caspase-9 and caspase-3 (Figure 5a), as well as caspase-9 and granzyme B (Figure 5b) in the lesions from CL patients. However, no correlation was observed between the expression of caspase-3 and granzyme B (Figure 5c), suggesting the activation of the mitochondrial pathway by granzyme B to induce cell death mechanisms in the samples.

The activation of cell death has been implicated in tissue damage observed in CL patients (Rethi and Eidsmo, 2012; Santos, Cda *et al.*, 2013). Thereafter, our next question was to investigate the relation between tissue injury and expression of caspase-9, caspase-3, and granzyme B. As shown in Figure 6, there was a positive correlation between protein expression of caspase-9 (Figure 6a), caspase-3 (Figure 6b), and granzyme B (Figure 6c) and the lesion size observed in CL patients. These data suggest the participation of cell death mechanism in tissue destruction observed in CL patients infected by *L. brazilienis*.

DISCUSSION

This study provides a global protein profiling comparison between lesions from CL patients and normal skin. We did not detect any *Leishmania* proteins in our proteomic analysis, possibly because of the scarce number of parasites in lesions caused by *L. braziliensis* (Bittencourt and Barral, 1991). We identified 59 proteins differently expressed between the samples; some of these proteins were identified only in the lesions from CL patients and other ones were unique in the normal skin. This fact does not mean that the proteins were not expressed in other samples, but it does suggest that they might be expressed to a significantly lesser extent or were posttranslational modified. The differences in the protein expressions were primarily associated with biological regulation of cell death, cell cycle, cell–cell signaling, immune response, and transport. The expression of the proteins such as TRB, upregulated in the lesions from CL patients, and IGBP1 and IL12RB1 unique to patients lesions,

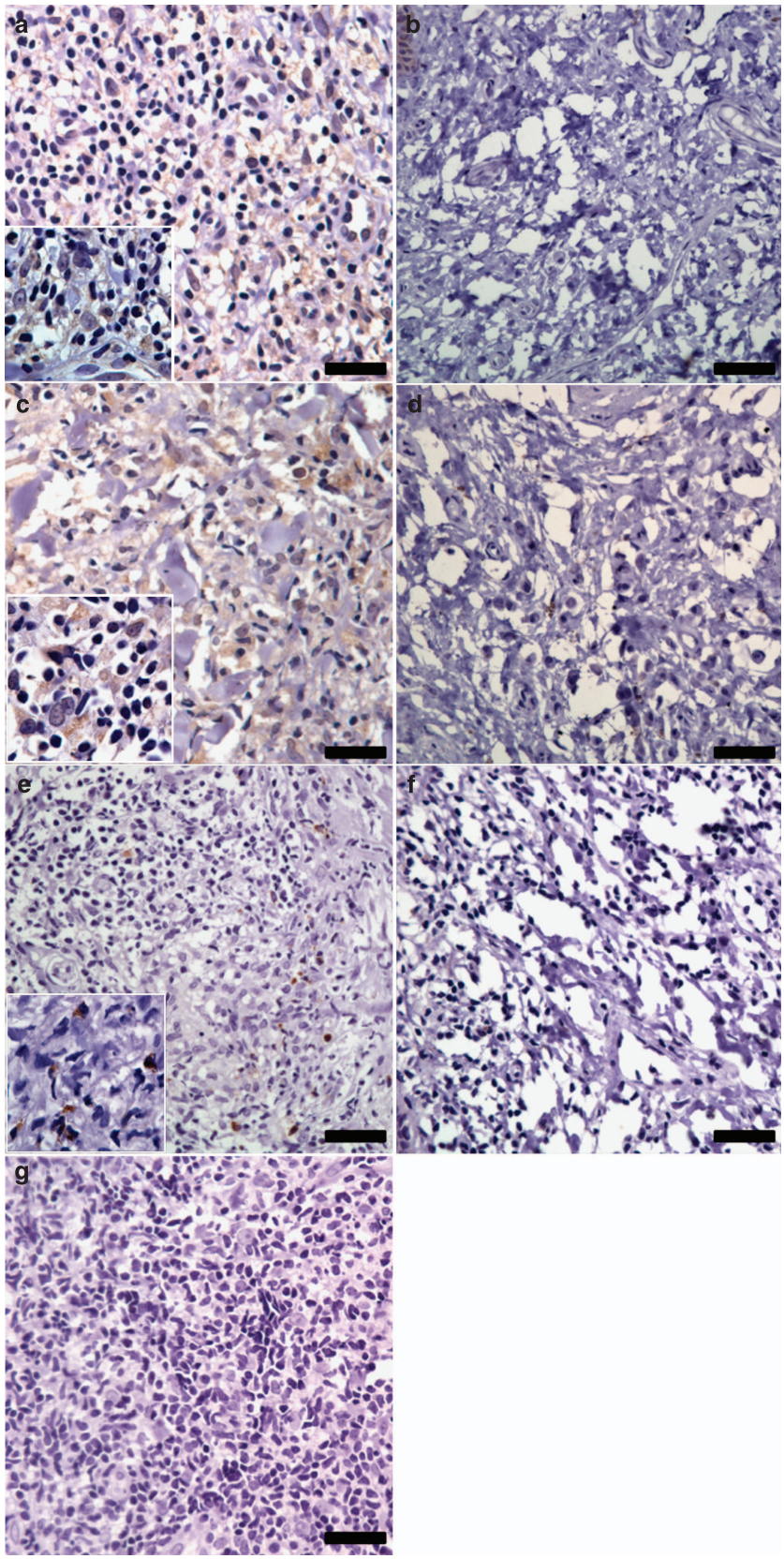

Figure 4. Immunohistochemistry for caspase-9, caspase-3, and granzyme B in samples. Tissue sections of cutaneous leishmaniasis (CL) patients ($n = 8$) were obtained and stained for (**a**) caspase-9, (**c**) caspase-3, and (**e**) granzyme B. Normal skin samples ($n = 3$) were immunostained for (**b**) caspase-9, (**d**) caspase-3, and (**f**) granzyme B. (**g**) Isotype control is shown. All samples were counterstained with hematoxylin and examined by light microscopy. Scale bar = 10 μm.

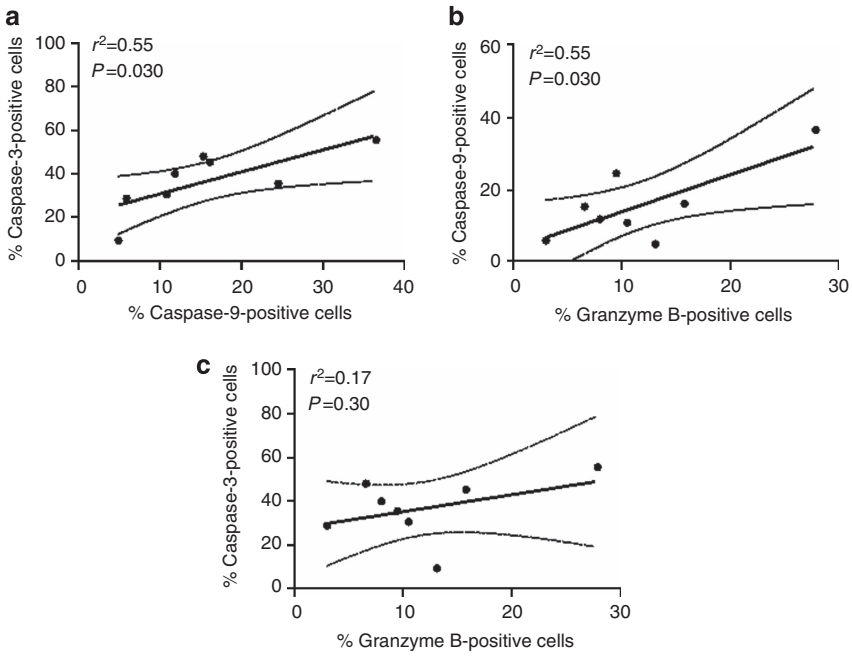

Figure 5. Correlation analysis between the protein expression in tissue from cutaneous leishmaniasis (CL) patients. Correlation analysis between the percentage of expression of (**a**) caspase-9 and granzyme B, (**b**) caspase-9 and caspase-3, and (**c**) caspase-3 and granzyme B in tissues from CL patients ($n=8$). Statistical comparisons were done using Spearman's (r^2) rank test. $P<0.05$ was considered significant.

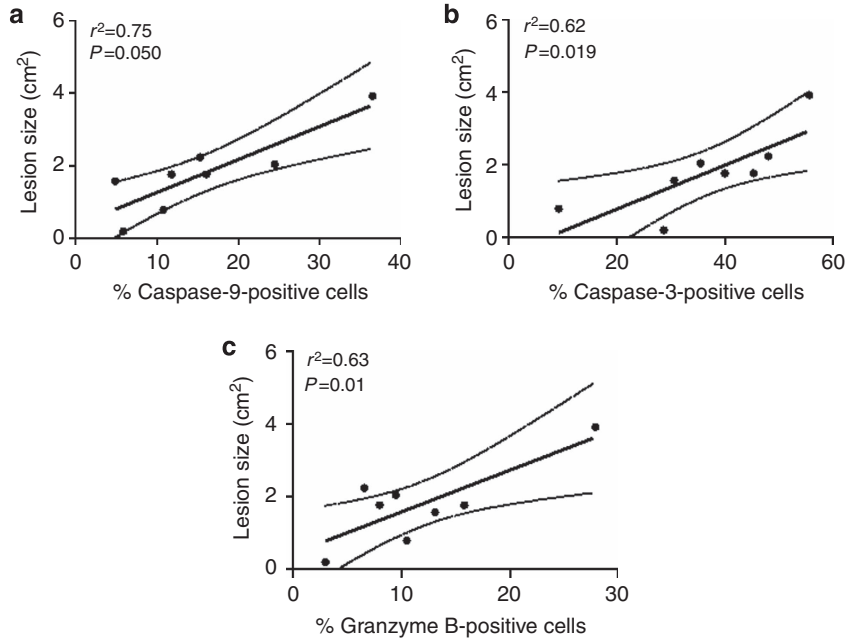

Figure 6. Correlation analysis between the protein expression and lesion size. Correlation analysis between the percentage of protein expression of (**a**) caspase-9, (**b**) caspase-3, and (**c**) granzyme B and lesion size of cutaneous leishmaniasis (CL) patients ($n=8$). Statistical comparisons were done using Spearman's (r^2) rank test. $P<0.05$ was considered significant.

which are known to affect activation of leukocytes (Germain, 2002; Staretz-Haham *et al.*, 2003; Sakashita *et al.*, 2011), may indicate the persistence of inflammation in the tissue (Clarêncio *et al.*, 2006; Kariminia *et al.*, 2007). Other identified proteins, CDK11A and NEK11, have been implicated in mitotic progression and DNA damage responses (Noguchi *et al.*, 2002; Shi *et al.*, 2009). It has been shown that proteins involved in cellular stress responses interact with and regulate signaling intermediates involved in the activation of innate and adaptive immune responses (Muralidharan and Mandrekar, 2013).

Large-scale analytical techniques based on functional proteomics generate an enormous amount of data, creating challenges for traditional methods of analysis (Gehlenborg *et al.*, 2010). Using biological network analysis, Cytoscape, and IPA-Ingenuity Systems, the differentially expressed proteins were organized in functional networks and potential canonical pathway. IL-23, TNFRI, caspase-3, caspase-8, and granzyme B were some of the proteins identified in the main network. Indeed, these molecules have already been described in different studies of *Leishmania* infection (Medeiros *et al.*, 2000; Carneiro *et al.*, 2009; Tolouei *et al.*, 2012; Novais *et al.*, 2013).

The activation of caspases results in cell death by apoptosis that can be induced by granzyme B through the activation of caspase-3 directly or through the mitochondrial pathway inducing activation of caspase-9 (Chávez-Galán *et al.*, 2009). Indeed, one of the proteins upregulated in the lesions from CL patients was caspase-9, being one of the central proteins found in the canonical pathway by IPA-Ingenuity Systems. Despite apoptosis being a programmed cell death mechanism associated with an anti-inflammatory immune response, studies in literature have implicated the activation of this pathway with tissue damage (Tasew *et al.*, 2010; Nylén and Eidsmo, 2012; Cevik *et al.*, 2013). In fact, in our histological evaluation, we observed areas of focal necrosis. Apoptotic cells can undergo secondary necrosis if not rapidly cleared by phagocytes, increasing the inflammatory response (Kono and Rock, 2008). In our study, positive correlations were observed between expression of caspase-9 and granzyme B and between caspase-9 and caspase-3. These data are strengthened by the association between the expression of caspase 9, caspase 3, and granzyme B and lesion size, displaying the participation of these proteins in tissue damage in CL caused by *L. braziliensis*. Indeed, our group demonstrated positive correlations between the intralesional CD8 T cell expressing granzyme B and the percentage of TUNEL-positive cells as well as the lesion size in CL patients (Santos, Cda *et al.*, 2013).

Taken together, this study showed an association of 59 identified proteins with biological regulation, including cell death. Upregulation of caspase-9 and the presence of caspase-3 and granzyme B in the lesions suggest participation of these proteins in the mechanisms associated with the progression of tissue damage observed in CL patients. We also observed the expression of the proteins that were not earlier described in the inflammatory site of CL. Therefore, our study provides a basis for further studies of pathogenesis of this disease.

MATERIALS AND METHODS

Clinical sample collection and preparation

Skin samples were obtained from the border of 11 biopsies from different CL patients before starting treatment. All patients lived in the municipality of Jiquiriça (State of Bahia, Brazil) and presented a single active lesion with 30 days of infection. CL is endemic in the state of Bahia, and Jiquiriça is one of the most important areas of *L. braziliensis* transmission (De Oliveira *et al.*, 2003). The diagnosis was made on the basis of clinical and histological characteristics of skin lesion compatible with CL plus a positive result in anti-leishmania delayed-type hypersensitivity or anti-leishmania serology. To confirm the diagnostic of CL, immunohistochemistry was performed for *Leishmania* analysis using anti-Leishmania IgG obtained in rabbits (see Immunohistochemistry section for more details; Supplementary Figure S3 online). None of the individuals had reported previous infection with *Leishmania*. All patients were submitted to the treatment with Glucantime (Safoni-Aventis, São Paulo, Brazil), and all lesions from CL patients healed after the treatment and there were not confounding medical conditions.

Normal skin samples ($n=6$) were obtained from healthy individuals by plastic surgery. For the proteomics study, six of these samples (three biopsies from CL patients and three from normal skin) were collected and cryopreserved. The samples were extracted directly in the rehydration buffer (8 M urea, 2% CHAPS, 0.28% dithiothreitol, 0.5% ampholites 3–10 pH gradient (immobilized pH gradient)), protease inhibitor (Amersham Biosciences, Uppsala, Sweden), and trace of Bromophenol blue at room temperature. After centrifugation, the supernatants were collected and quantified using the Bradford assay. The remaining samples (8 biopsies from CL patients and 3 from normal skin) were fixed in 10% formalin-buffered solution, embedded in paraffin, and used for the immunohistochemical analyses. This study had ethical permit approval from Centro de Pesquisas Gonçalo Moniz (CPqGM/FIOCRUZ-Bahia), in adherence to the Declaration of Helsinki Principles. Institutional Review Board approval was obtained and all participants or their legal guardians gave their written consent before entering the study.

All subjects consented by written agreement to inclusion in this study.

2DE and detection of differentially expressed proteins

Samples were subjected to isoelectric focusing using immobilized pH gradient Dry Strips with immobilized pH gradient, pH range 3–10, 18 cm, linear (GE Healthcare). Samples were applied by in-gel rehydration technique. Isoelectric focusing was performed in the Ethan IPGphor instrument (GE Healthcare, Uppsala, Sweden) according to the following protocol: rehydration, 10 hours, 50 V; 3 hours, 1,000 V; 1 hour, 8,000 V; 10 hours or to 50,000 Vh. After isoelectric focusing, strips were equilibrated in 50 mM Tris-HCl, pH 8.8, 6 M urea, 2.0% SDS, 30% glycerol with 10 mM dithiothreitol for 10 minutes, and then for 10 minutes in the same buffer without dithiothreitol but with 20 mM iodoacetamide. The second-dimensional SDS-PAGE was performed in an Ettan Dalt Six (GE Healthcare). Triplicate 2D gels were generated for each sample, with 9 gels representing lesions and 9 gels representing normal skin samples to ensure reproducibility. Generated gels were stained with silver nitrate. Spot detection and quantification were done using the Image Master Platinum v6.0 GE Healthcare software. Student's *t*-test was used to ensure statistical significance of the spot selection ($P<0.05$). Proteins from the two groups of samples (CL lesions and normal skin) that showed change in expression pattern between lesion and normal skin samples by >2-fold of the spot volume or were unique were taken for identification by matrix-assisted laser desorption/ionization time-of-flight MS.

Protein identification

Protein spots were excised from the gels and subjected to in-gel trypsin digestion using a μC18 ZipTip (Millipore Billerica, MA) followed by MS analysis by the matrix-assisted laser desorption/

ionization time-of-flight MS on Micromass M@LDI-Reflectron instrument (Waters, Milford, MA). Embedded Micromass software (MassLynx Software v4.0) was used to process the mass spectra. Peptide spectra were internally calibrated using autolytic peptides from the trypsin (842.510, 1,045.564, and 2,211.105 Da). To identify proteins, we performed searches in the NCBI nr sequence database using the ProFound search engine (http://prowl.rockefeller.edu/prowl-cgi/profound.exe). One missed cleavage, alkylation with iodoacetamide, and partial oxidation of methionine were allowed. Search parameters were set on mass tolerance <0.1 Da, isoelectric point, and molecular weight as compared with the migration position of a spot in the 2D gel, and ''*Homo sapiens*'' was selected for species search. Significance of the identification was evaluated according to the different parameters, included a probability value that means that a protein identified in a database is the one that was analyzed on the basis of experimental conditions, isoelectric point, and molecular weight of the protein. We also used *Z*-score, a statistical distribution estimated when the search result is compared with an estimated random match population. Under these statistical analyses, the higher value of *Z*-score means the higher is the probability that a particular protein is not caused by random coincidence. Besides that, significance was also evaluated by total number of identified peptides for the protein matched and sequence coverage of predicted peptides.

Biological network analysis

Protein names were translated into Gene Ontology terms (Lewis *et al.*, 2000). Biological network analysis of obtained data was performed using GoMiner (http://discover.nci.nih.gov/gominer/) (Zeeberg *et al.*, 2003), Cytoscape v2.8.1 (http://www.cytoscape.org) (Shannon *et al.*, 2003; Smoot *et al.*, 2011), and Ingenuity System Pathway Analysis program v9.0 (IPA-Ingenuity Systems, Redwood City, CA). GoMiner provides classification of identified proteins into biologically coherent categories and assesses these categories. Cytoscape is an open source software platform for building and analysis of biological interaction networks. The network was analyzed based on topological parameters such as number of nodes and neighborhood connectivity using a Cytoscape plug-in called ''*Network Analyzer*'' (Assenov *et al.*, 2008). In a given network, each gene is represented as a node, and the interactions between the nodes are defined as edges. MiMIplugin (http://mimiplugin.ncibi.org/) (Saito *et al.*, 2012) was used to extract relevant proteins and RNAs from public databases. Network modules were extracted by MCODE v.2.1 tool (Saito *et al.*, 2012). IPA-Ingenuity Systems was employed to model the possible canonical pathway/function and network involving the 59 proteins identified. Fisher's exact test was used to calculate the *P*-value determining the network connectivity.

Immunohistochemistry

Formalin-fixed and paraffin-embedded tissue specimen sections (5 μm) were obtained, and immunohistochemistry was performed as described previously. The following primary antibodies were used: caspase-3 (ab4051; 1:200), caspase-9 (ab63342; 1:200), granzyme B (ab134933; 1:50) (all from Abcam, Cambridge, UK), and anti-*Leishmania* IgG obtained in rabbit (1:1,000). The specimens were then incubated in sequence with biotinylated secondary antibody, streptavidin–peroxidase complex (LSAB + System-HRP; Dako, São Paulo, Brazil). The slides were visualized by 3,3′-diaminobenzidine chromogen and counterstained with hematoxylin. Isotype control antibody (R&D Systems, Abengdon, UK) was used as negative controls. Staining cells were counted as 1,000 cells distributed in five different microscopic fields with a magnification power of $\times 400$. Digital images of tissue sections were captured using a Nikon E600 light microscope and a Q-Color 1 Olympus (Melville, NY) digital camera. Quantification of stained areas was performed using Image Pro-Plus software (Media Cybernetics, Rockville, MD). Spearman's correlation analysis tests were also applied. Analyses were conducted using GraphPrism 5 software (GraphPad Software, San Diego, CA), and a $P<0.05$ was considered significant.

CONFLICT OF INTEREST

The authors state no conflict of interest.

ACKNOWLEDGMENTS

We are grateful to all patients and control subjects who participated in this study. This study was supported by grants from Fundação de Amparo a Pesquisa do Estado da Bahia (FAPESB) e/Conselho Nacional de Desenvolvimento Científico e Tecnológico (CNPq grant number PPSUS SUS0025/2009) and from Pronex (FAPESB/CNPq grant 738712006). CSS received fellowships from Coordenação de Aperfeiçoamento de Pessoal de Nível Superior (CAPES), Brazil, and Conselho Nacional de Desenvolvimento Científico e Tecnológico (CNPq)/Programa Ciencias sem Fronteiras; CIB and MB-N are senior investigators of CNPq. SS is grateful to Oves Minnesfond for support and encouragement. The work in the Souchelnytskyi group is supported in part by grants from the Radiumhemmet research funds (121202), the Swedish Cancer Society, the Swedish Research Council, the Swedish Institute, INTAS, Erasmus KI-UWM, and STINT.

SUPPLEMENTARY MATERIAL

Supplementary material is linked to the online version of the paper at http://www.nature.com/jid

REFERENCES

Assenov Y, Ramírez F, Schelhorn S-E *et al.* (2008) Computing topological parameters of biological networks. *Bioinformatics* 24:282–4

Bittencourt AL, Barral A (1991) Evaluation of the histopathological classifications of American cutaneous and mucocutaneous leishmaniasis. *Mem Inst Oswaldo Cruz* 86:51–6

Carneiro FP, De Magalhães AV, De Jesus Abreu Almeida Couto M *et al.* (2009) Foxp3 expression in lesions of the different clinical forms of American tegumentary leishmaniasis. *Parasite Immunol* 31:646–51

Carvalho LP, Passos S, Schriefer A *et al.* (2012) Protective and pathologic immune responses in human tegumentary leishmaniasis. *Front Immunol* 3:301

Cevik O, Adiguzel Z, Baykal AT *et al.* (2013) The apoptotic actions of platelets in acute ischemic stroke. *Mol Biol Rep* 40:6721–7

Chávez-Galán L, Arenas-Del Angel MC, Zenteno E *et al.* (2009) Cell death mechanisms induced by cytotoxic lymphocytes. *Cell Mol Immunol* 6:15–25

Clarêncio J, de Oliveira CI, Bomfim G *et al.* (2006) Characterization of the T-cell receptor Vbeta repertoire in the human immune response against Leishmania parasites. *Infect Immun* 74:4757–65

De Oliveira CI, Báfica A, Oliveira F *et al.* (2003) Clinical utility of polymerase chain reaction-based detection of Leishmania in the diagnosis of American cutaneous leishmaniasis. *Clin Infect Dis* 37:e149–53

Faria DR, Souza PEA, Durães FV *et al.* (2009) Recruitment of CD8(+) T cells expressing granzyme A is associated with lesion progression in human cutaneous leishmaniasis. *Parasite Immunol* 31:432–9

Forgber M, Basu R, Roychoudhury K *et al.* (2006) Mapping the antigenicity of the parasites in Leishmania donovani infection by proteome serology. *PLoS One* 1:e40

Gehlenborg N, O'Donoghue SI, Baliga NS *et al.* (2010) Visualization of omics data for systems biology. *Nat Methods* 7:S56–68

Germain RN (2002) T-cell development and the CD4-CD8 lineage decision. *Nat Rev Immunol* 2:309–22

Haudek VJ, Slany A, Gundacker NC *et al.* (2009) Proteome maps of the main human peripheral blood constituents. *J Proteome Res* 8:3834–43

Javad F, Day PJR (2012) Protein profiling of keloidal scar tissue. *Arch Dermatol Res* 304:533–40

Kariminia A, Bourreau E, Ronet C *et al.* (2007) Selective expression of the V beta 14 T cell receptor on Leishmania guyanensis–specific CD8 + T cells during human infection. *J Infect Dis* 195:739–47

Kedzierski L (2010) Leishmaniasis vaccine: where are we today? *J Glob Infect Dis* 2:177–85

Keesen TSL, Antonelli LRV, Faria DR *et al.* (2011) CD4(+) T cells defined by their Vβ T cell receptor expression are associated with immunoregulatory profiles and lesion size in human leishmaniasis. *Clin Exp Immunol* 165:338–51

Kestler HA, Müller A, Gress TM *et al.* (2005) Generalized Venn diagrams: a new method of visualizing complex genetic set relations. *Bioinformatics* 21:1592–5

Kono H, Rock KL (2008) How dying cells alert the immune system to danger. *Nat Rev Immunol* 8:279–89

Lewis S, Ashburner M, Reese MG (2000) Annotating eukaryote genomes. *Curr Opin Struct Biol* 10:349–54

Lord SJ, Rajotte RV, Korbutt GS *et al.* (2003) Granzyme B: a natural born killer. *Immunol Rev* 193:31–8

Matrangolo FSV, Liarte DB, Andrade LC *et al.* (2013) Comparative proteomic analysis of antimony-resistant and -susceptible Leishmania braziliensis and Leishmania infantum chagasi lines. *Mol Biochem Parasitol* 190: 63–75

Medeiros IM, Reed S, Castelo A *et al.* (2000) Circulating levels of sTNFR and discrepancy between cytotoxicity and immunoreactivity of TNF-alpha in patients with visceral leishmaniasis. *Clin Microbiol Infect* 6: 34–7

Menezes JPB, Almeida TF, Petersen A L.O. A. *et al.* (2013) Proteomic analysis reveals differentially expressed proteins in macrophages infected with Leishmania amazonensis or Leishmania major. *Microbes Infect* 15: 579–91

Muralidharan S, Mandrekar P (2013) Cellular stress response and innate immune signaling: integrating pathways in host defense and inflammation. *J Leukoc Biol* 94:1167–84

Noguchi K, Fukazawa H, Murakami Y *et al.* (2002) Nek11, a new member of the NIMA family of kinases, involved in DNA replication and genotoxic stress responses. *J Biol Chem* 277:39655–65

Novais FO, Carvalho LP, Graff JW *et al.* (2013) Cytotoxic T cells mediate pathology and metastasis in cutaneous leishmaniasis. *PLoS Pathog* 9:e1003504

Nylén S, Eidsmo L (2012) Tissue damage and immunity in cutaneous leishmaniasis. *Parasite Immunol* 34:551–61

Ong CT, Khoo YT, Mukhopadhyay A *et al.* (2010) Comparative proteomic analysis between normal skin and keloid scar. *Br J Dermatol* 162: 1302–15

Rethi B, Eidsmo L (2012) FasL and TRAIL signaling in the skin during cutaneous leishmaniasis - implications for tissue immunopathology and infectious control. *Front Immunol* 3:163

Rukmangadachar LA, Kataria J, Hariprasad G *et al.* (2011) Two-dimensional difference gel electrophoresis (DIGE) analysis of sera from visceral leishmaniasis patients. *Clin Proteomics* 8:4

Saito R, Smoot ME, Ono K *et al.* (2012) A travel guide to Cytoscape plugins. *Nat Methods* 9:1069–76

Sakashita S, Li D, Nashima N *et al.* (2011) Overexpression of immunoglobulin (CD79a) binding protein1 (IGBP-1) in small lung adenocarcinomas and its clinicopathological significance. *Pathol Int* 61:130–7

Santos, Cda S, Boaventura V, Ribeiro Cardoso C *et al.* (2013) CD8(+) granzyme B(+)-mediated tissue injury vs. CD4(+)IFNγ(+)-mediated parasite killing in human cutaneous leishmaniasis. *J Invest Dermatol* 133:1533–40

Shannon P, Markiel A, Ozier O *et al.* (2003) Cytoscape: a software environment for integrated models of biomolecular interaction networks. *Genome Res* 13:2498–504

Shi J, Hershey JWB, Nelson MA (2009) Phosphorylation of the eukaryotic initiation factor 3f by cyclin-dependent kinase 11 during apoptosis. *FEBS Lett* 583:971–7

Smoot ME, Ono K, Ruscheinski J *et al.* (2011) Cytoscape 2.8: new features for data integration and network visualization. *Bioinformatics* 27:431–2

Staretz-Haham O, Melamed R, Lifshitz M *et al.* (2003) Interleukin-12 receptor beta1 deficiency presenting as recurrent Salmonella infection. *Clin Infect Dis* 37:137–40

Tasew G, Nylén S, Lieke T *et al.* (2010) Systemic FasL and TRAIL neutralisation reduce leishmaniasis induced skin ulceration. *PLoS Negl Trop Dis* 4: e844

Tolouei S., Ghaedi K., Khamesipour A. *et al.* (2012) IL-23 and IL-27 levels in macrophages collected from peripheral blood of patients with healing vs non-healing form of cutaneous leishmaniasis. *Iran J Parasitol* 7:18–25

Zeeberg BR, Feng W, Wang G *et al.* (2003) GoMiner: a resource for biological interpretation of genomic and proteomic data. *Genome Biol* 4:R28